Journal of Mathematical Modeling
Vol. 3, No. 2, 2016, pp. 145-167

JMM

Effects of Hall current and ion-slip on unsteady hydromagnetic generalised Couette flow in a rotating Darcian channel

Jitendra Kumar Singh*, Shaik Ghousia Begum and Naveen Joshi

Department of Mathematics, V. S. K. University, Bellary-583105, India
Emails: s.jitendrak@yahoo.com, ghousiacc@gmail.com, joshi.naveen94@gmail.com

Abstract. Unsteady hydromagnetic generalised Couette flow of a viscous, incompressible and electrically conducting fluid between two horizontal parallel porous plates Darcian channel in the presence of a uniform transverse magnetic field taking Hall current and ion-slip into account in a rotating system is investigated. An exact solution of the governing equations is obtained by Laplace transform technique. The expression for the shear stress at the moving porous plate due to primary and secondary flows is also derived. Asymptotic behavior of the solution is analyzed at the start-up and final stage of the motion to gain some physical insight into the flow pattern. Numerical values of primary and secondary velocities and that of shear stress at the moving porous plate of the channel due to primary and secondary flows are displayed graphically for various values of different flow parameters.

Keywords: Hall current, ion-slip, rotation, permeability, suction/injection.
AMS Subject Classification: 76U05, 76W05.

1 Introduction

Investigation of problems of unsteady hydromagnetic Couette flow of a viscous, incompressible and electrically conducting fluid in a rotating system

*Corresponding author.
Received: 26 June 2015 / Revised: 13 August 2015 / Accepted: 13 August 2015.

permeated by a uniform transverse magnetic field has been an attractive topic of research during past several decades due to its varied and wide ranging applications in the areas of astrophysics, geophysics and fluid engineering problems. Magnitude analysis shows that Coriolis force is more significant than that of viscous and inertial forces in hydromagnetic equations of motion in a rotating system and is comparable in magnitude to the magnetic force. Therefore, the study of combined effects of rotation and magnetic field on hydromagnetic fluid flow problems becomes more relevant. Taking into account the importance of such study Hide and Roberts [19], Nanda and Mohanty [27], Debnath [11,12], Seth and Jana [33], Sarojamma and Krishna [29], Prasad Rao *et al.* [28], Seth *et al.* [30–32, 34–36], Chandran *et al.* [7], Singh *et al.* [39], Singh [37], Hayat *et al.* [16–18], Wang and Hayat [42], Beg *et al.* [5], Das *et al.* [10], Guria *et al.* [14], Makinde *et al.* [23], Jha and Apere [20, 22], Guchhait *et al.* [13], Chauhan and Agrawal [8], Singh and Pathak [38], Ahmed and Chamkha [2] and Sulochana [41] studied MHD flow in a rotating medium considering different aspects of the problem. Study of MHD flow between parallel porous plates is important because it may have applications in many biological, agricultural and engineering problems such as designing of cooling systems with liquid metals, nuclear reactor using liquid metal coolant, geothermal energy extraction, underground energy transport, blood flow problems etc. Keeping in view the importance of such investigations Mishra and Muduli [26], Prasad Rao *et al.* [28], Abbas *et al.* [1], Hayat *et al.* [15], Beg *et al.* [6], Seth et al. [30–32, 35, 36], Guchhait et al. [13], Jha and Apere [21] and Ahmed and Chamkha [2] studied hydromagnetic flow between porous boundaries considering different aspects of the problem. When an ionized fluid with low density is permeated by a strong magnetic field, there acts a force, called Lorentz force. Due to this force fluid particles start spiraling about magnetic lines of force instead of moving on a circular path prior to collision with the other fluid particles. An electric current is induced due to the spiraling of fluid particles about magnetic lines of force, called Hall current and this current is mutually perpendicular to electric and magnetic fields. Furthermore, for same electromagnetic force, the motion of ions is different from electrons and so the diffusion velocity of electrons is much larger than that of ions. Usually, we are considering the electric current density determined by the diffusion velocity of the electrons. However, when the magnetic field is very strong the diffusion velocity of ions may not be negligible (Cramer and Pai [9]). In this condition study of combined effects of Hall current and ion-slip become important. Hall current and ion-slip play a vital role in determining the flow features of fluid flows.

Hall current and ion-slip is likely to be important in MHD power generation, nuclear power reactors, underground energy storage systems, magneto meters, Hall effect sensors, spacecraft propulsion and several areas of astrophysics and geophysics. Soundalgekar *et al.* [40], Attia [3], Beg *et al.* [6] and Jha and Apere [20,22] studied combined effects of Hall current and ion-slip under different conditions and configurations. Flow through a porous medium (Bear [4]) is analyzed using Darcy-Forchheimer drag force model which includes both bulk matrix and porous drag and second order inertial impedance. Investigation of MHD fluid flow problems through a Darcian channel is important because of its wide applications in biological, geophysical and technological problems. Chauhan and Agrawal [8] studied effects of Hall current on steady MHD Couette flow in a rotating channel partially filled with a porous medium. Transient Couette flow in a rotating non-Darcian porous medium parallel plate configuration is investigated by Beg *et al.* [5]. Beg et al. [6] studied combined effects of Hall current and ion-slip on unsteady MHD Hartmann-Couette flow within a Darcian channel using network numerical solutions. Singh and Pathak [38] investigated effects of rotation and Hall current on mixed convection MHD flow through porous medium filled in a vertical channel in presence of thermal radiation. Sulochana [41] studied effects of Hall current and rotation on unsteady MHD three dimensional flows through porous medium in the presence of an inclined magnetic field. An exact solution of Hartmann Newtonian radiating MHD flow for a rotating vertical porous channel immersed in a Darcian porous regime is carried-out by Ahmed and Chamkha [2].

The aim of present investigation is to study the effects of Hall current and ion-slip on unsteady hydromagnetic generalized Couette flow in a rotating Darcian channel. Fluid flow within a channel is induced due to impulsive movement of the upper plate of the channel as well as by applied pressure gradient acting along the longitudinal axis of the plates of the channel and is permeated by a uniform transverse magnetic field which is fixed relative to the stationary plate. Laplace transform technique is used to obtain an exact solution of the problem.

2 Mathematical model of the problem and its solution

Consider the unsteady flow of a viscous, incompressible and electrically conducting fluid between two parallel porous plates Darcian channel $y = -h$ and $y = h$ in the presence of a uniform transverse magnetic field B_0 applied parallel to y-axis. The fluid as well as the plates of the Darcian channel

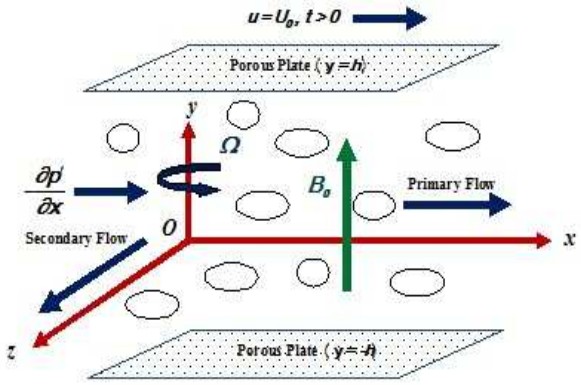

Figure 1: Geometry of the physical problem.

rotates in unison as rigid body rotation with uniform angular velocity $\overrightarrow{\Omega}$ about y-axis. Initially (i.e. when time $t \leq 0$), fluid and plates of the channel are assumed to be at rest. At time $t > 0$, upper plate $y = h$ starts moving with uniform velocity U_0 in x-direction while the lower plate $y = -h$ is kept fixed. A pressure gradient $-\partial p'/\partial x$ is applied along the longitudinal axis of the plates of the channel i.e. along x-axis. Suction/injection takes place through the porous walls of the channel with uniform transpiration velocity V_o ($V_0 > 0$ for suction and $V_0 < 0$ for injection). Geometry of the physical problem is shown in the Fig. 1. It is assumed that no applied or polarization voltages exist so induced electric field $\overrightarrow{E} = (0, 0, 0)$. This is because no energy is being added or extracted from fluid by electrical means (Meyer [25]). It may be noted that the magnetic Reynolds number is very small for metallic liquids and partially ionized fluids so induced magnetic field produced by fluid motion is negligible in comparison to applied one (Cramer and Pai [9]). Since the plates of the channel are of infinite extent in x and z-directions, so all the physical quantities except pressure will be function of y and t only. Therefore, fluid velocity $\overrightarrow{V}$ and magnetic field $\overrightarrow{B}$ are given by

$$\overrightarrow{V} = (u, V_0, w), \quad \overrightarrow{B} = (0, B_0, 0), \tag{1}$$

where u and w are the fluid velocities in x and z-directions respectively.

Under the above assumptions, the governing equations for hydromagnetic fluid flow of a viscous, incompressible and electrically conducting fluid in a rotating Darcian channel taking Hall current and ion-slip in to account,

are given by

$$\frac{\partial u}{\partial t}+V_0\frac{\partial u}{\partial y}+2w\Omega=-\frac{1}{\rho}\frac{\partial p}{\partial x}+\nu\frac{\partial^2 u}{\partial y^2}-\frac{\sigma B_0^2}{\rho}\left[\frac{u(1+B_iB_e)+wB_e}{(1+B_iB_e)^2+B_e^2}\right]-\frac{\nu u}{k}, \quad (2)$$

$$0=-\frac{1}{\rho}\frac{\partial p}{\partial y}, \quad (3)$$

$$\frac{\partial w}{\partial t}+V_0\frac{\partial w}{\partial y}-2u\Omega=\nu\frac{\partial^2 w}{\partial y^2}+\frac{\sigma B_0^2}{\rho}\left[\frac{uB_e-w(1+B_iB_e)}{(1+B_iB_e)^2+B_e^2}\right]-\frac{\nu w}{k}, \quad (4)$$

where $\nu, \sigma, \rho, B_e, B_i, p$ and k are, respectively, kinematic coefficient of viscosity, electrical conductivity of fluid, fluid density, Hall current parameter, ion-slip parameter, modified pressure including centrifugal force and magnetic pressure and permeability of the porous medium.

Eq. (3) shows that modified pressure p is constant along y-axis i.e. along axis of rotation. The pressure gradient term is absent in Eq. (4) because there is a net cross flow in z-direction.

The initial and boundary conditions for fluid flows are

$$u=w=0 \quad \text{for} \quad -h\le y\le h \quad \text{and} \quad t\le 0, \quad (5)$$

$$u=w=0 \quad \text{at} \quad y=-h \quad \text{for} \quad t>0, \quad (6)$$

$$u=U_0, \quad w=0 \quad \text{at} \quad y=h \quad \text{for} \quad t>0. \quad (7)$$

The mathematical model of the present physical problem is governed by Eqs. (2) and (4) subject to the initial condition (5) and boundary conditions (6) and (7). We have to find the solution of Eqs. (2) and (4) subject to the initial condition (5) and boundary conditions (6) and (7). Writing Eqs. (2) and (4) in compact form, we obtain

$$\frac{\partial q}{\partial t}+V_0\frac{\partial q}{\partial y}-2i\Omega q=-\frac{1}{\rho}\frac{\partial p}{\partial x}+\nu\frac{\partial^2 q}{\partial y^2}-\frac{\sigma B_0^2}{\rho}\left[\frac{(1+B_iB_e)-iB_e}{(1+B_iB_e)^2+B_e^2}\right]q-\frac{\nu q}{k}, \quad (8)$$

where $q=u+iw$.

The initial condition (5) and boundary conditions (6) and (7), in compact form become

$$q=0 \quad \text{for} \quad -h\le y\le h \quad \text{and} \quad t\le 0, \quad (9)$$

$$q=0 \quad \text{at} \quad y=-h \quad \text{for} \quad t>0, \quad (10)$$

$$q=U_0 \quad \text{at} \quad y=h \quad \text{for} \quad t>0. \quad (11)$$

Introducing dimensionless variables $x^* = \frac{x}{h}, y^* = \frac{y}{h}$, $p^* = \frac{p}{\rho {U_0}^2}$, $q_i^* = \frac{q}{U_0} = u_i^* + iw_i^*$ and $t^* = \frac{tU_0}{h}$, Eq. (8) in dimensionless form, becomes

$$\begin{cases} \frac{\partial q_i^*}{\partial t^*} + N_t \frac{\partial q_i^*}{\partial y^*} - 2iK^2 q_i^* = -R + \frac{1}{R_e}\frac{\partial^2 q_i^*}{\partial {y^*}^2} - \frac{H_a^2}{R_e}\left[\frac{(1+B_iB_e)-iB_e}{(1+B_iB_e)^2+B_e^2}\right] q_i^* \\ -\frac{q_i^*}{D_a R_e}, \end{cases} \tag{12}$$

where $N_t = \frac{V_0}{U_0}$ is suction/injection parameter ($N_t > 0$ for suction and $N_t < 0$ for injection) which represents the mass of fluid passing into the Darcian channel via the stationary plate and exiting via the moving plate, $K^2 = \frac{\Omega h}{U_0}$ is rotation parameter which represents the relative strength of Coriolis force to the inertial force, $R = \frac{dp^*}{dx^*}$ is modified pressure gradient, $R_e = \frac{U_0 h}{\nu}$ is Reynolds number which represents the relative strength of inertial force to the viscous force, $H_a^2 = \frac{\sigma B_0^2 h^2}{\mu}$ is square of Hartmann number which represents the relative strength of magnetic force to the viscous force and $D_a = \frac{k}{h^2}$ is Darcy number (permeability parameter) which represents the relative permeability of Darcian channel.

The initial and boundary conditions (9) to (11), in dimensionless form, are

$$q_i^* = 0 \quad \text{for} \quad -1 \le y^* \le 1 \quad \text{and} \quad t^* \le 0, \tag{13}$$

$$q_i^* = 0 \quad \text{at} \quad y^* = -1 \quad \text{for} \quad t^* > 0, \tag{14}$$

$$q_i^* = 1 \quad \text{at} \quad y^* = 1 \quad \text{for} \quad t^* > 0. \tag{15}$$

Using Laplace transform, Eq. (12) with the help of initial condition (13), assumes the form

$$\begin{cases} \frac{d^2\overline{q_i^*}}{{dy^*}^2} - N_t R_e \frac{d\overline{q_i^*}}{dy^*} - \Big[sR_e + \frac{1}{D_a} + \frac{H_a^2(1+B_iB_e)}{((1+B_iB_e)^2+B_e^2)} \\ \qquad -i\Big\{2K^2R_e + \frac{H_a^2 B_e}{((1+B_iB_e)^2+B_e^2)}\Big\}\Big]\overline{q_i^*} = \frac{RR_e}{s}, \end{cases} \tag{16}$$

where $\overline{q_i^*}(y^*, s) = \int_0^\infty e^{-st} q_i^*(y^*, t^*) dt^*$, $s > 0$ and s being Laplace transform parameter.

The boundary conditions (14) and (15) after using Laplace transform, become

$$\overline{q_i^*} = 0 \quad \text{at} \quad y^* = -1, \tag{17}$$

$$\overline{q_i^*} = \frac{1}{s} \quad \text{at} \quad y^* = 1. \tag{18}$$

Solution of Eq. (16) subject to boundary conditions (17) and (18) is given by

$$\begin{cases} \overline{q_i^*} = \sum_{n=0}^{\infty}\left[\frac{1}{s}\left(e^{-a\lambda_1} - e^{-b\lambda_1}\right) + \frac{(-1)^n R}{s(s+m-iM)}\left(e^{-c\lambda_1} + e^{-d\lambda_1}\right)\right] \\ -\frac{R}{s(s+m-iM)}, \end{cases} \tag{19}$$

where

$$\begin{cases} a = 4n+1-y^*, b = 4n+3+y^*, c = 2n+1-y^*, d = 2n+1+y^*, \\ m = \frac{1}{D_a R_e} + \frac{H_a^2(1+B_iB_e)}{R_e\left((1+B_iB_e)^2+B_e^2\right)}, \\ M = 2K^2 + \frac{H_a^2 B_e}{R_e\left((1+B_iB_e)^2+B_e^2\right)}, \\ \lambda_1 = \left(\frac{N_t R_e}{2}\right) + \sqrt{Re}\sqrt{s + \left(\frac{N_t^2 R_e}{4}\right) + m - iM}. \end{cases} \tag{20}$$

Taking inverse Laplace transform of Eq. (19), solution for the velocity field is expressed in the following form (McLachlan [24]).

$$\begin{cases} q_i^*(y^*,t^*) = \frac{1}{2}\sum_{n=0}^{\infty}\Big[\Big\{e^{-aP_1}erfc\left(\frac{a\sqrt{R_e}}{2\sqrt{t^*}} - P\sqrt{t^*}\right) \\ +e^{-aP_2}erfc\left(\frac{a\sqrt{R_e}}{2\sqrt{t^*}} + P\sqrt{t^*}\right) - e^{-bP_1}erfc\left(\frac{b\sqrt{R_e}}{2\sqrt{t^*}} - P\sqrt{t^*}\right) \\ -e^{-bP_2}erfc\left(\frac{b\sqrt{R_e}}{2\sqrt{t^*}} + P\sqrt{t^*}\right)\Big\} \\ +\frac{(-1)^n R(m+iM)}{(m^2+M^2)}\Big\{e^{-cP_1} \times erfc\left(\frac{c\sqrt{R_e}}{2\sqrt{t^*}} - P\sqrt{t^*}\right) \\ +e^{-cP_2}erfc\left(\frac{c\sqrt{R_e}}{2\sqrt{t^*}} + P\sqrt{t^*}\right) + e^{-dP_1}erfc\left(\frac{d\sqrt{R_e}}{2\sqrt{t^*}} - P\sqrt{t^*}\right) \\ +e^{-dP_2}erfc\left(\frac{d\sqrt{R_e}}{2\sqrt{t^*}} + P\sqrt{t^*}\right)\Big\} \\ -e^{(m-iM)t^*}\Big\{e^{-cN_tR_e}erfc\left(\frac{c\sqrt{R_e}}{2\sqrt{t^*}} - \frac{N_t}{2}\sqrt{R_e t^*}\right) \\ +e^{-dN_tR_e}erfc\left(\frac{d\sqrt{R_e}}{2\sqrt{t^*}} - \frac{N_t}{2}\sqrt{R_e t^*}\right) + erfc\left(\frac{c\sqrt{R_e}}{2\sqrt{t^*}} + \frac{N_t}{2}\sqrt{R_e t^*}\right) \\ +erfc\left(\frac{d\sqrt{R_e}}{2\sqrt{t^*}} + \frac{N_t}{2}\sqrt{R_e t^*}\right)\Big\}\Big\}\Big] - \frac{R(m+iM)}{(m^2+M^2)}\Big[1 - e^{-(m-iM)t^*}\Big], \end{cases} \tag{21}$$

where

$$\begin{cases} X_1 = \frac{N_t^2 R_e}{4} + m, \quad \alpha,\beta = \frac{1}{\sqrt{2}}\Big[\Big\{(X_1)^2 + M^2\Big\}^{\frac{1}{2}} \pm X_1\Big]^{\frac{1}{2}}, \\ P = \alpha - i\beta, \quad P_1 = \frac{N_t R_e}{2} + P\sqrt{R_e}, \quad P_2 = \frac{N_t R_e}{2} - P\sqrt{R_e}. \end{cases} \tag{22}$$

Eq. (21) represents the general solution for hydromagnetic generalized Couette flow within a rotating Darcian channel with Hall current and ion-slip effects.

3 Shear stress at the moving porous plate

The dimensionless shear stress components τ_{xi}^* and τ_{zi}^* at the moving porous plate $y^* = 1$ due to primary and secondary flows are given by

$$\begin{cases} (\tau_{xi}^* + i\tau_{zi}^*)|_{y^*=1} = \frac{1}{2}\sum_{n=0}^{\infty}\Big[P_1\Big\{e^{-a'P_1}erfc\left(\frac{a'\sqrt{R_e}}{2\sqrt{t^*}} - P\sqrt{t^*}\right) \\ -e^{-b'P_1}erfc\left(\frac{b'\sqrt{R_e}}{2\sqrt{t^*}} - P\sqrt{t^*}\right)\Big\} + P_2\Big\{e^{-a'P_2}erfc\left(\frac{a'\sqrt{R_e}}{2\sqrt{t^*}} + P\sqrt{t^*}\right) \\ -e^{-b'P_2}erfc\left(\frac{b'\sqrt{R_e}}{2\sqrt{t^*}} + P\sqrt{t^*}\right)\Big\} + 2\sqrt{\frac{R_e}{\pi t^*}}\Big\{e^{-\left(\frac{a'^2R_e}{4t^*} + \frac{a'N_tR_e}{2} + P^2t^*\right)} \\ -e^{-\left(\frac{b'^2R_e}{4t^*} + \frac{b'N_tR_e}{2} + P^2t^*\right)} \\ +\frac{(-1)^n R(m+iM)}{(m^2+M^2)}\Big\{P_1\Big\{e^{-c'P_1}erfc\left(\frac{c'\sqrt{R_e}}{2\sqrt{t^*}} - P\sqrt{t^*}\right) \\ +e^{-d'P_1}erfc\left(\frac{d'\sqrt{R_e}}{2\sqrt{t^*}} - P\sqrt{t^*}\right)\Big\} + P_2\Big\{e^{-c'P_2}erfc\left(\frac{c'\sqrt{R_e}}{2\sqrt{t^*}} + P\sqrt{t^*}\right) \\ +e^{-d'P_2}erfc\left(\frac{d'\sqrt{R_e}}{2\sqrt{t^*}} + P\sqrt{t^*}\right)\Big\} + 2\sqrt{\frac{R_e}{\pi t^*}}\Big\{e^{-\left(\frac{c'^2R_e}{4t^*} + \frac{c'N_tR_e}{2} + P^2t^*\right)} \\ +e^{-\left(\frac{d'^2R_e}{4t^*} + \frac{d'N_tR_e}{2} + P^2t^*\right)}\Big\} \\ -e^{-(m-iM)t^*}\Big\{N_tR_e\Big\{e^{-c'N_tR_e}erfc\left(\frac{c'\sqrt{R_e}}{2\sqrt{t^*}} - \frac{N_t\sqrt{R_et^*}}{2}\right) \\ +e^{-d'N_tR_e}erfc\left(\frac{d'\sqrt{R_e}}{2\sqrt{t^*}} - \frac{N_t\sqrt{R_et^*}}{2}\right)\Big\} \\ +2\sqrt{\frac{R_e}{\pi t^*}}\Big\{e^{-\left(\frac{c'^2R_e}{4t^*} + \frac{c'N_tR_e}{2} + \frac{N_t^2R_et^*}{4}\right)} + e^{-\left(\frac{d'^2R_e}{4t^*} + \frac{d'N_tR_e}{2} + \frac{N_t^2R_et^*}{4}\right)}\Big\}\Big\}\Big\}\Big], \end{cases} \tag{23}$$

where $a' = 4n, \quad b' = 4n+4, \quad c' = 2n \quad$ and $\quad d' = 2n+2.$

4 Asymptotic solutions

Asymptotic behavior of the solution (21) is analyzed at the start-up stage (i.e. $t^* << 1$) and final stage (i.e. $t^* >> 1$) of the motion to gain some physical insight into the flow pattern.

CASE-1: At the start-up stage of motion (i.e. $t^* \ll 1$)

Primary velocity u_i^* and secondary velocity w_i^*, which are obtained from

the general solution (21) for small values of time t^*, are given by

$$\begin{cases} u_i^* = -Rt^* + \sum_{n=0}^{\infty}\Big[e^{-\frac{aN_tR_e}{2}}\Big\{\Big(1+\frac{a^2R_eX_1}{2}\Big)erfc\left(\frac{a\sqrt{R_e}}{2\sqrt{t^*}}\right) \\ -\sqrt{\frac{R_et^*}{\pi}}aX_1e^{-\frac{a^2R_e}{4t^*}}\Big\} - e^{-\frac{bN_tR_e}{2}}\Big\{\Big(1+\frac{b^2R_eX_1}{2}\Big)erfc\left(\frac{b\sqrt{R_e}}{2\sqrt{t^*}}\right) \\ -\sqrt{\frac{R_et^*}{\pi}}bX_1e^{-\frac{b^2R_e}{4t^*}}\Big\} \\ +(-1)^nR\Big\{e^{-\frac{cN_tR_e}{2}}\Big\{t^*+(1+X_1t^*)\frac{c^2R_e}{2}+\frac{c^4R_e^2X_1}{12}\Big\}erfc\left(\frac{c\sqrt{R_e}}{2\sqrt{t^*}}\right) \\ +e^{-\frac{dN_tR_e}{2}}\Big\{t^*+(1+X_1t^*)\frac{d^2R_e}{2}+\frac{d^4R_e^2X_1}{12}\Big\}erfc\left(\frac{d\sqrt{R_e}}{2\sqrt{t^*}}\right) \\ -\sqrt{\frac{R_et^*}{\pi}}\Big\{ce^{-\frac{cN_tR_e}{2}}\Big\{\frac{2t^*X_1}{3}+\Big(1-\frac{c^2R_eX_1}{6}\Big)\Big\}e^{-\frac{c^2R_e}{4t^*}} \\ +de^{-\frac{cN_tR_e}{2}}\Big\{\frac{2t^*X_1}{3}+\Big(1-\frac{d^2R_eX_1}{6}\Big)\Big\}e^{-\frac{d^2R_e}{4t^*}}\Big\}\Big\}\Big], \end{cases} \tag{24}$$

$$\begin{cases} w_i^* = M\sum_{n=0}^{\infty}\Big[e^{-\frac{aN_tR_e}{2}}\Big\{-\frac{a^2R_e}{2}erfc\left(\frac{a}{2}\sqrt{\frac{R_e}{t^*}}\right)+a\sqrt{\frac{R_et^*}{\pi}}e^{-\frac{a^2R_e}{4t^*}}\Big\} \\ -e^{-\frac{bN_tR_e}{2}}\Big\{-\frac{b^2R_e}{2}erfc\left(\frac{b}{2}\sqrt{\frac{R_e}{t^*}}\right)+b\sqrt{\frac{R_et^*}{\pi}}e^{-\frac{b^2R_e}{4t^*}}\Big\} \\ -(-1)^nR\Big\{e^{-\frac{cN_tR_e}{2}}\Big\{\Big(t^*+\frac{c^2R_e}{6}\Big)\frac{c^2R_e}{2}erfc\left(\frac{c}{2}\sqrt{\frac{R_e}{t^*}}\right) \\ -\Big(2t^*+\frac{c^2R_e}{2}\Big)\frac{c}{3}\sqrt{\frac{R_et^*}{\pi}}e^{-\frac{c^2R_e}{4t^*}}\Big\} \\ +e^{-\frac{dN_tR_e}{2}}\Big\{\Big(t^*+\frac{d^2R_e}{6}\Big)\frac{d^2R_e}{2}erfc\left(\frac{d}{2}\sqrt{\frac{R_e}{t^*}}\right) \\ +\Big(2t^*+\frac{d^2R_e}{2}\Big)\frac{d}{3}\sqrt{\frac{R_et^*}{\pi}}e^{-\frac{d^2R_e}{4t^*}}\Big\}\Big\}\Big]. \end{cases} \tag{25}$$

It is clear from the expressions (24) and (25) that, their arises Rayleigh boundary layer of thickness $O(\sqrt{t^*})$ in the vicinity of the moving porous plate $y^* = 1$ due to initial impulsive movement of the upper plate, at the starting stage. It is also noticed from expressions (24) and (25) that the primary velocity u_i^* is independent of rotation whereas secondary velocity w_i^* is independent of permeability. The primary velocity u_i^* has significant effects of Hall current, ion-slip, magnetic field and permeability whereas the secondary velocity w_i^* has significant effects of Hall current, ion-slip, rotation and magnetic field. However both the primary and secondary velocities are considerably affected by suction/injection. There are no inertial oscillations in the flow-field up to this stage.

CASE-2: At the final stage of motion (i.e. $t^* \gg 1$)

In this case the expressions for primary velocity u_i^* and secondary velocity w_i^*, which are obtained from the general solution (21), are represented in the following forms

$$u_i^*(y^*,t^*) = u_{is}^*(y^*) + u_{it}^*(y^*,t^*), \tag{26}$$

$$w_i^*(y^*,t^*) = w_{is}^*(y^*) + w_{it}^*(y^*,t^*), \tag{27}$$

where

$$\begin{cases} u_{is}^* = -\frac{Rm}{m^2+M^2} + \sum_{n=0}^{\infty}\Big[\Big\{e^{-a\left(\frac{N_tR_e}{2}+\alpha\sqrt{R_e}\right)}\cos(a\beta\sqrt{R_e}) \\ -e^{-b\left(\frac{N_tR_e}{2}+\alpha\sqrt{R_e}\right)}\cos(b\beta\sqrt{R_e})\Big\} \\ +\frac{(-1)^nR}{(m^2+M^2)}\Big\{e^{-c\left(\frac{N_tR_e}{2}+\alpha\sqrt{R_e}\right)}\left(m\cos(c\beta\sqrt{R_e}) - M\sin(c\beta\sqrt{R_e})\right) \\ +e^{-d\left(\frac{N_tR_e}{2}+\alpha\sqrt{R_e}\right)}\left(m\cos(d\beta\sqrt{R_e}) - M\sin(d\beta\sqrt{R_e})\right)\Big\}\Big], \end{cases} \tag{28}$$

$$\begin{cases} w_{is}^* = -\frac{RM}{m^2+M^2} + \sum_{n=0}^{\infty}\Big[\Big\{e^{-a\left(\frac{N_tR_e}{2}+\alpha\sqrt{R_e}\right)}\sin(a\beta\sqrt{R_e}) \\ -e^{-b\left(\frac{N_tR_e}{2}+\alpha\sqrt{R_e}\right)}\sin(b\beta\sqrt{R_e})\Big\} \\ +\frac{(-1)^nR}{(m^2+M^2)}\Big\{e^{-c\left(\frac{N_tR_e}{2}+\alpha\sqrt{R_e}\right)}\left(m\sin(c\beta\sqrt{R_e}) + M\cos(c\beta\sqrt{R_e})\right) \\ +e^{-d\left(\frac{N_tR_e}{2}+\alpha\sqrt{R_e}\right)}\left(m\sin(d\beta\sqrt{R_e}) + M\cos(d\beta\sqrt{R_e})\right)\Big\}\Big], \end{cases} \tag{29}$$

$$u_{it}^*(y^*,t^*) = u_{it_1}^*(y^*,t^*) + u_{it_2}^*(y^*,t^*), \tag{30}$$

$$\begin{cases} u_{it_1}^* = \frac{e^{-X_1t^*}}{2}\sum_{n=0}^{\infty}\Big[(\eta_1-\eta_2) + \frac{(-1)^nR}{(m^2+M^2)}\Big\{m(\eta_3+\eta_5) \\ -M(\eta_4+\eta_6) - 4\sqrt{\frac{R_et^*}{\pi}}\eta_7\Big\}\Big], \end{cases} \tag{31}$$

$$\begin{cases} u_{it_2}^* = \frac{Re^{-mt^*}}{(m^2+M^2)}\left(m\cos(Mt^*) - M\sin(Mt^*)\right) \\ \times\Big[1 - \sum_{n=0}^{\infty}(-1)^n(e^{-cN_tR_e} + e^{-dN_tR_e})\Big], \end{cases} \tag{32}$$

$$w_{it}^*(y^*,t^*) = w_{it_1}^*(y^*,t^*) + w_{it_2}^*(y^*,t^*), \tag{33}$$

$$\begin{cases} w_{it_1}^* = \frac{e^{-X_1t^*}}{2}\sum_{n=0}^{\infty}\Big[(\eta_8-\eta_9) + \frac{(-1)^nR}{(m^2+M^2)}\Big\{m(\eta_4+\eta_6) \\ +M(\eta_3+\eta_5) - 4\sqrt{\frac{R_et^*}{\pi}}\eta_{10}\Big\}\Big], \end{cases} \tag{34}$$

$$\begin{cases} w^*_{it_2} = \frac{Re^{-mt^*}}{(m^2+M^2)}\left(m\sin(Mt^*) + M\cos(Mt^*)\right) \\ \times\Big[1 - \sum_{n=0}^{\infty}(-1)^n(e^{-cN_tR_e} + e^{-dN_tR_e})\Big], \end{cases} \tag{35}$$

$$\begin{cases} \eta_1 = a\sqrt{\frac{R_e}{\pi t^*}}\frac{e^{-(\frac{a^2R_e}{4t^*}+\frac{aN_tR_e}{2})}}{\psi_1}\Big[\Big(\frac{a^2R_e}{4t^*} - X_1t^*\Big)\cos(Mt^*) + (Mt^*)\sin(Mt^*)\Big], \\ \eta_2 = b\sqrt{\frac{R_e}{\pi t^*}}\frac{e^{-(\frac{b^2R_e}{4t^*}+\frac{bN_tR_e}{2})}}{\psi_2}\Big[\Big(\frac{b^2R_e}{4t^*} - X_1t^*\Big)\cos(Mt^*) + (Mt^*)\sin(Mt^*)\Big], \\ \eta_3 = c\sqrt{\frac{R_e}{\pi t^*}}\frac{e^{-(\frac{c^2R_e}{4t^*}+\frac{cN_tR_e}{2})}}{\psi_3}\Big[\Big(\frac{c^2R_e}{4t^*} - X_1t^*\Big)\cos(Mt^*) + (Mt^*)\sin(Mt^*)\Big], \\ \eta_4 = c\sqrt{\frac{R_e}{\pi t^*}}\frac{e^{-(\frac{c^2R_e}{4t^*}+\frac{cN_tR_e}{2})}}{\psi_3}\Big[\Big(\frac{c^2R_e}{4t^*} - X_1t^*\Big)\sin(Mt^*) - (Mt^*)\cos(Mt^*)\Big], \\ \eta_5 = d\sqrt{\frac{R_e}{\pi t^*}}\frac{e^{-(\frac{d^2R_e}{4t^*}+\frac{dN_tR_e}{2})}}{\psi_4}\Big[\Big(\frac{d^2R_e}{4t^*} - X_1t^*\Big)\cos(Mt^*) + (Mt^*)\sin(Mt^*)\Big], \\ \eta_6 = d\sqrt{\frac{R_e}{\pi t^*}}\frac{e^{-(\frac{d^2R_e}{4t^*}+\frac{dN_tR_e}{2})}}{\psi_4}\Big[\Big(\frac{d^2R_e}{4t^*} - X_1t^*\Big)\sin(Mt^*) - (Mt^*)\cos(Mt^*)\Big], \\ \eta_7 = \Big\{\frac{ce^{-\left(\frac{c^2R_e}{4t^*}+\frac{cN_tR_e}{2}\right)}}{(c^2R_e - N_t^2R_et^{*2})} + \frac{de^{-\left(\frac{d^2R_e}{4t^*}+\frac{dN_tR_e}{2}\right)}}{(d^2R_e - N_t^2R_et^{*2})}\Big\}(m\cos(Mt^*) - M\sin(Mt^*)), \\ \eta_8 = a\sqrt{\frac{R_e}{\pi t^*}}\frac{e^{-\left(\frac{a^2R_e}{4t^*}+\frac{aN_tR_e}{2}\right)}}{\psi_1}\Big[\Big(\frac{a^2R_e}{4t^*} - X_1t^*\Big)\sin(Mt^*) - (Mt^*)\cos(Mt^*)\Big], \\ \eta_9 = b\sqrt{\frac{R_e}{\pi t^*}}\frac{e^{-\left(\frac{b^2R_e}{4t^*}+\frac{bN_tR_e}{2}\right)}}{\psi_2}\Big[\Big(\frac{b^2R_e}{4t^*} - X_1t^*\Big)\sin(Mt^*) - (Mt^*)\cos(Mt^*)\Big], \\ \eta_{10} = \Big\{\frac{ce^{-\left(\frac{c^2R_e}{4t^*}+\frac{cN_tR_e}{2}\right)}}{(c^2R_e - N_t^2R_et^{*2})} + \frac{de^{-\left(\frac{d^2R_e}{4t^*}+\frac{dN_tR_e}{2}\right)}}{(d^2R_e - N_t^2R_et^{*2})}\Big\}(m\sin(Mt^*) + M\cos(Mt^*)), \\ \psi_1 = \Big(\frac{a^2R_e}{4t^*} - X_1t^*\Big)^2 + (Mt^*)^2, \quad \psi_2 = \Big(\frac{b^2R_e}{4t^*} - X_1t^*\Big)^2 + (Mt^*)^2, \\ \psi_3 = \Big(\frac{c^2R_e}{4t^*} - X_1t^*\Big)^2 + (Mt^*)^2, \quad \psi_4 = \Big(\frac{d^2R_e}{4t^*} - X_1t^*\Big)^2 + (Mt^*)^2. \end{cases}$$

For large values of time t^*, it is seen from the expressions (26) and (27) that flow-field is in quasi-steady state. Steady flows represented by $u^*_{is}(y^*)$ and $w^*_{is}(y^*)$ are confined within a thin modified Ekman-Hartmann boundary layer of thickness $O(((\frac{N_tR_e}{2}) + \alpha\sqrt{R_e})^{-1})$. It is noticed from Eq. (22) that α decreases on increasing D_a whereas it increases on increasing H_a^2 which implies that the thickness of modified Ekman-Hartmann boundary layer increases on increasing D_a whereas it decreases on increasing H_a^2. Boundary layer thickness profiles are depicted for various values of B_e, B_i, K^2 and N_t and are represented in Figs. 2 and 3. It is observed from Fig. 2 that the thickness of modified Ekman-Hartmann boundary layer increases on increasing both B_e and B_i. It is evident from Fig. 3 that the thickness

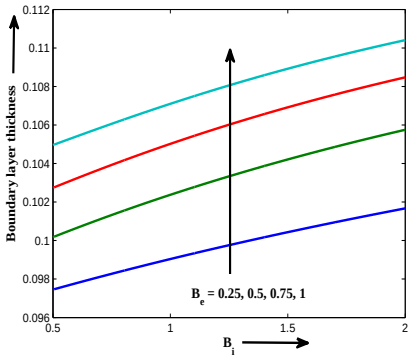

Figure 2: Boundary layer thickness profiles when $K^2 = 1, H_a^2 = 25, D_a = 1.0$ and $N_t = 2.0$.

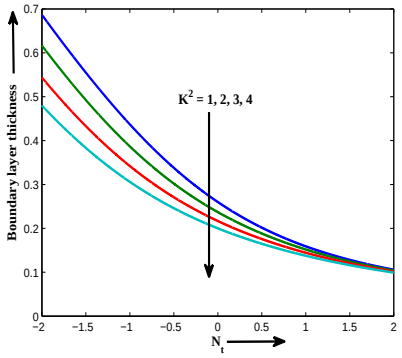

Figure 3: Boundary layer thickness profiles when $B_i = 2.0, B_e = 0.5, H_a^2 = 25$ and $D_a = 1.0$.

of modified Ekman-Hartmann boundary layer decreases on increasing both K^2 and $N_t(> 0)$ and it increases on increasing $N_t(< 0)$.

It is also observed from Eqs. (28) and (29) that steady flow executes spatial oscillations in the flow-field excited by Hall current, ion-slip, rotation, magnetic field, permeability and suction/injection. It is evident from expressions (30) to (35) that unsteady flow exhibits inertial oscillation in the flow-field excited by Hall current, ion-slip, rotation and magnetic field. It is also demonstrated from Eqs. (30) to (35) that unsteady flow, represented by $u_{it}^*(y^*, t^*)$ and $w_{it}^*(y^*, t^*)$ are divided into two parts viz. $u_{it_1}^*(y^*, t^*), w_{it_1}^*(y^*, t^*)$ and $u_{it_2}^*(y^*, t^*), w_{it_2}^*(y^*, t^*)$. The inertial oscillations in $u_{it_1}^*(y^*, t^*)$ and $w_{it_1}^*(y^*, t^*)$ damped out effectively in dimensionless time of $O(X_1^{-1})$, whereas that in $u_{it_2}^*(y^*, t^*)$ and $w_{it_2}^*(y^*, t^*)$ damped out effectively in dimensionless time of $O(m^{-1})$ when the final steady state is developed. This shows that suction/injection tends to reduce time of decay of inertial oscillations in the major part of unsteady flow. It may be noted that in absence of suction/injection, time of decay of inertial oscillations in the unsteady flow is enhanced due to presence of Hall current, ion-slip and permeability. It is also seen from Eqs. (30) to (35) that, even in the absence of both Hall current and rotation, there are no inertial oscillations in the flow-field. This implies that both the Hall current and rotation induced inertial oscillations in the flow-field for large values of time t^*. This result is in agreement with the result obtained by Seth *et al.* [36].

5 Results and discussion

To study the effects of Hall current, ion-slip, rotation, magnetic field, permeability, suction/injection and time on the flow-field, the numerical values of the primary and secondary fluid velocities, computed from the analytical solution (21), are depicted graphically versus channel width variable y^* and are represented in Figs. 4-10 for various values of Hall current parameter B_e, ion-slip parameter B_i, rotation parameter K^2, magnetic parameter H_a^2, Darcy number D_a, suction/injection parameter N_t and time t^* taking pressure gradient $R = 5$ and Reynolds number $R_e = 4$ which is valid for Darcian model. Fig. 4 demonstrates the effect of Hall current on the primary velocity u_i^* and secondary velocity w_i^*. It is revealed from Fig. 4 that both the primary velocity u_i^* and secondary velocity w_i^* increase on increasing B_e. This implies that the Hall current tends to enhance fluid flow in both primary and secondary flow directions. This is due to the fact that Hall current induces secondary flow in the flow-field. Fig. 5 represents the influence of ion-slip on the primary velocity u_i^* and secondary velocity w_i^*. It is observed from Fig. 5 that the primary velocity u_i^* increases whereas the secondary velocity w_i^* decreases on increasing B_i. This shows that the ion-slip tends to enhance fluid flow in primary flow direction whereas it has reverse effect on the fluid flow in secondary flow direction. Fig. 6 shows the effect of rotation on the primary velocity u_i^* and secondary velocity w_i^*. It is revealed from Fig. 6 that the primary velocity u_i^* decreases whereas secondary velocity w_i^* increases on increasing K^2. Since K^2 represents the ratio of Coriolis force to inertia force, an increase in K^2 implies the increase in the strength of Coriolis force. In a rotating system Coriolis force is generated due to rotation whose tendency is to suppress primary flow and to induce secondary flow into the flow-field. Thus, rotation tends to retard fluid flow in the primary flow direction whereas it has a reverse effect on fluid flow in the secondary flow direction which is also characteristics of Hall current. Fig. 7 depicts the effect of magnetic field on the primary velocity u_i^* and secondary velocity w_i^*. It is evident from Fig. 7 that both the primary velocity u_i^* and secondary velocity w_i^* decrease on increasing H_a^2 which implies that magnetic field tends to retard fluid flow in both the primary and secondary flow directions. This is due to the fact that when an electrically conducting fluid flows in the presence of a magnetic field, a mechanical force, known as Lorentz force, is generated in the flow-field whose tendency is to resist fluid flow. Fig. 8 displays the influence of permeability on the primary velocity u_i^* and secondary velocity w_i^*. It is observed from Fig. 8 that both the primary velocity u_i^* and secondary velocity w_i^* increase on increasing D_a. This implies that permeability tends

to enhance fluid flow in both primary and secondary flow directions. Fig. 9 demonstrates the effect of suction/injection on the primary velocity u_i^* and secondary velocity w_i^*. It is revealed from Fig. 9 that the primary velocity u_i^* increases on increasing $N_t(> 0)$ and decreases on increasing $N_t(< 0)$ whereas the secondary velocity w_i^* is oscillatory in nature on increasing N_t. This implies suction tends to enhance fluid flow in primary flow direction whereas injection has reverse effect on it and fluid flow in secondary flow direction is oscillatory in nature due to suction/injection. Fig. 10 depicts the effect of time on the primary velocity u_i^* and secondary velocity w_i^*. It is evident from Fig. 10 that the primary velocity u_i^* increases on increasing t^* when $0.25 \leq t^* \leq 0.50$, attains its maximum and again decreases on increasing t^* when $0.50 < t^* \leq 1.0$ whereas the secondary velocity w_i^* increases on increasing t^*. This implies that the fluid flow in the primary flow direction is getting enhanced as time progresses when $0.25 \leq t^* \leq 0.50$ whereas it has reverse effect on the fluid flow in primary flow direction when $0.50 < t^* \leq 1.0$. Fluid flow in secondary flow direction is enhanced as time passes. There exists a cross flow in the vicinity of the moving plate of the channel due to impulsive movement of the upper plate.

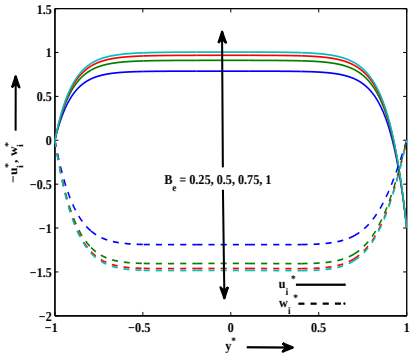

Figure 4: Velocity profiles when $B_i = 2.0, K^2 = 1, H_a^2 = 25, D_a = 1.0, N_t = 2.0$ and $t^* = 0.25$.

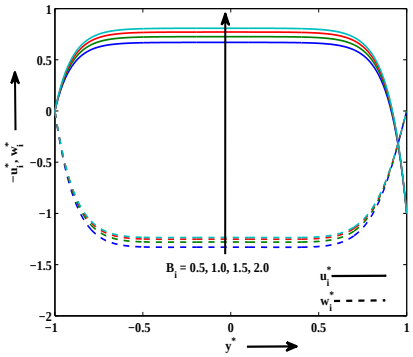

Figure 5: Velocity profiles when $B_e = 0.5, K^2 = 1, H_a^2 = 25, D_a = 1.0, N_t = 2.0$ and $t^* = 0.25$.

The numerical values of dimensionless shear stress at the moving plate due to the primary and secondary flows computed from the analytical expression (23), are presented graphically in Figs. 11 - 14 for various values of $B_e, B_i, K^2, H_a^2, D_a, N_t, t^*$ and R taking $R_e = 4$. It is found from Fig. 11 that the primary shear stress τ_{xi}^* decreases whereas the secondary shear stress τ_{zi}^* increases on increasing B_e. Both the primary shear stress τ_{xi}^* and secondary shear stress τ_{zi}^* increase on increasing B_i. This implies that Hall

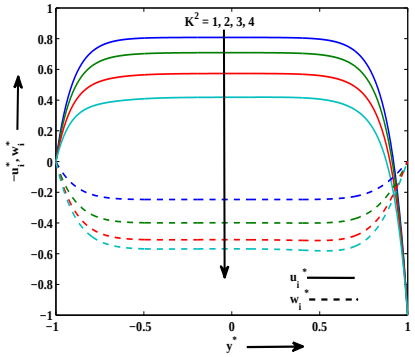

Figure 6: Velocity profiles when $B_e = 0.5, B_i = 2.0, H_a^2 = 25, D_a = 1.0, N_t = 2.0$ and $t^* = 0.25$.

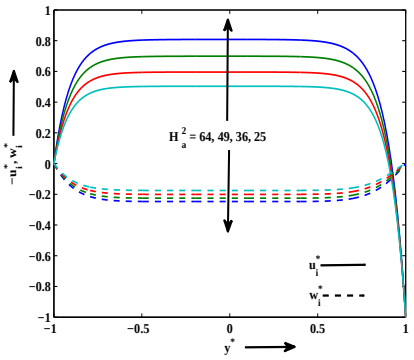

Figure 7: Velocity profiles when $B_e = 0.5, B_i = 2.0, K^2 = 1, D_a = 1.0, N_t = 2.0$ and $t^* = 0.25$.

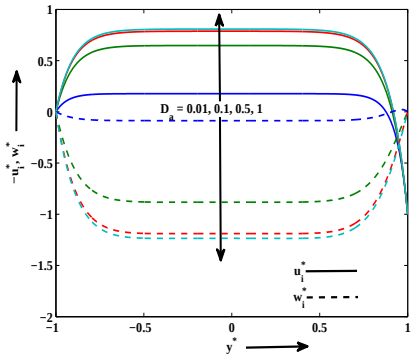

Figure 8: Velocity profiles when $B_e = 0.5, B_i = 2.0, K^2 = 1, H_a^2 = 25, N_t = 2.0$ and $t^* = 0.25$.

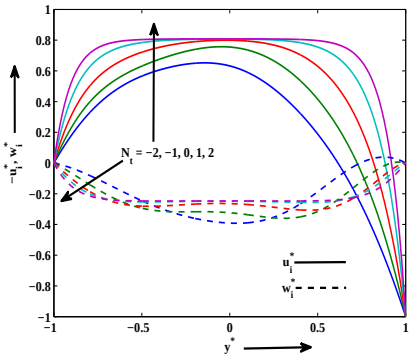

Figure 9: Velocity profiles when $B_e = 0.5, B_i = 2.0, K^2 = 1, H_a^2 = 25, D_a = 1.0$ and $t^* = 0.25$.

current tends to reduce primary shear stress at the moving plate whereas it has reverse effect on the secondary shear stress at the moving plate. Ion-slip tends to enhance both the primary and secondary shear stresses at the moving plate. It is observed from Fig. 12 that both the primary shear stress τ_{xi}^* and secondary shear stress τ_{zi}^* decrease on increasing K^2. The primary shear stress τ_{xi}^* increases on increasing H_a^2 whereas the secondary shear stress τ_{zi}^* decreases on increasing H_a^2 when $1 \leq K^2 \leq 3$ and it increases on increasing H_a^2 when $3 < K^2 \leq 4$. This implies that rotation tends to reduce both the primary and secondary shear stresses at the moving plate.

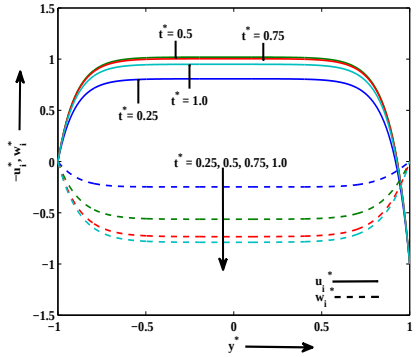

Figure 10: Velocity profiles when $B_e = 0.5, B_i = 2.0, K^2 = 1, H_a^2 = 25, D_a = 1.0$ and $N_t = 2.0$.

Magnetic field tends to enhance primary shear stress at the moving plate and secondary shear stress at the moving plate when $3 < K^2 \leq 4$ whereas it has reverse effect on the secondary shear stress at the moving plate when $1 \leq K^2 \leq 3$. It is revealed from Fig. 13 that the primary shear stress τ_{xi}^* decreases whereas secondary shear stress τ_{zi}^* increases on increasing D_a which implies that permeability tends to reduce primary shear stress at the moving plate whereas it has reverse effect on the secondary shear stress at the moving plate. It is observed from Fig. 14 that both the primary shear stress τ_{xi}^* and secondary shear stress τ_{zi}^* increases on increasing t^* as well as R. This implies that both the time and pressure gradient tend to enhance both the primary and secondary shear stresses at the moving plate.

To compare our results with the results obtained by Beg *et al.* [6], we have drawn velocity profiles at the centre of the channel versus time t^* for various values of D_a taking $B_e = 3, B_i = 3, K^2 = 0, H_a^2 = 100, N_t = 1, R = 5$ and $R_e = 5$ and are presented in Figs. 15 and 16. It is observed from Figs. 15 and 16 that both the primary velocity u_i^* and secondary velocity w_i^* increase on increasing D_a at the centre of the channel. We also note that the steady state attained considerably quicker with strongest Darcian drag force (lower D_a value, $D_a = 0.01$). This is in agreement with the result obtained by Beg *et al.* [6] using network numerical solution method.

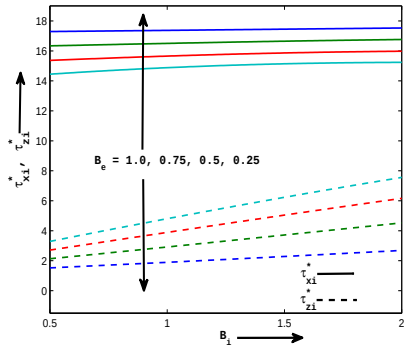

Figure 11: Shear stress profiles when $K^2 = 1, H_a^2 = 25, D_a = 1.0, N_t = 2.0, t^* = 0.25$ and $R = 5$.

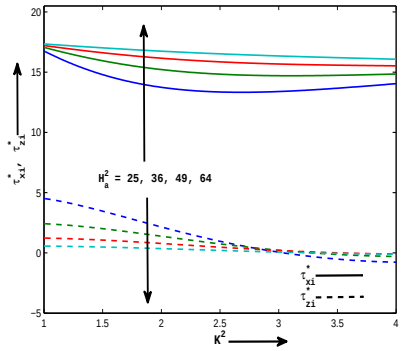

Figure 12: Shear stress profiles when $B_e = 0.5, B_i = 2.0, D_a = 1.0, N_t = 2.0, t^* = 0.25$ and $R = 5$.

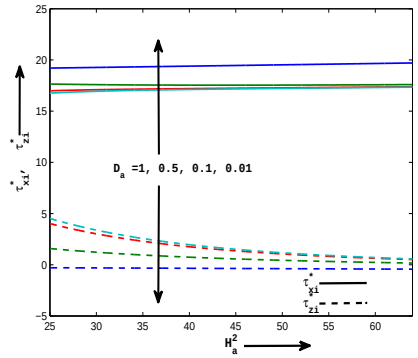

Figure 13: Shear stress profiles when $B_e = 0.5, B_i = 2.0, K^2 = 1, N_t = 2.0, t^* = 0.25$ and $R = 5$.

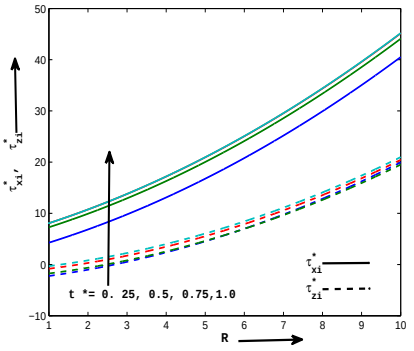

Figure 14: Shear stress profiles when $B_e = 0.5, B_i = 2.0, K^2 = 1, H_a^2 = 25, D_a = 1.0$ and $N_t = 2.0$.

6 Conclusion

In present investigation the effects of Hall current and ion-slip on unsteady hydromagnetic generalized Couette flow in a rotating Darcian channel is studied. Significant outcomes are summarized below:

For small values of time t^*, their arises Rayleigh boundary layer in the vicinity of the moving plate. It is also noticed that the primary velocity is independent of rotation whereas secondary velocity is independent of

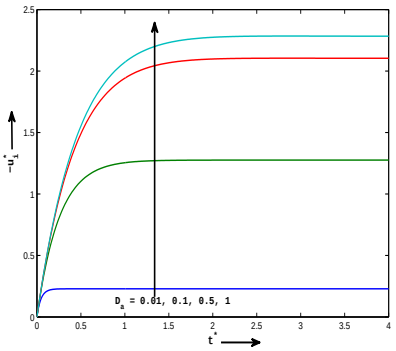

Figure 15: Primary velocity profiles.

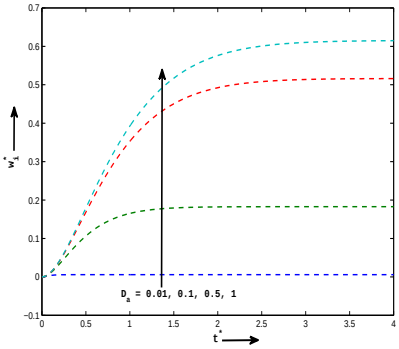

Figure 16: Secondary velocity profiles.

permeability. The primary velocity has significant effects of Hall current, ion-slip, magnetic field and permeability whereas the secondary velocity has significant effects of Hall current, ion-slip, rotation and magnetic field. However both the primary and secondary velocities are considerably affected by suction/injection. For large values of time t^*, flow-field is in quasi-steady state. Steady flow is confined within a thin modified Ekman-Hartmann boundary layer. It is also seen that steady flow executes spatial oscillations in the flow-field excited by Hall current, ion-slip, rotation, magnetic field, permeability and suction/injection. Unsteady flow exhibits inertial oscillation in the flow-field excited by Hall current and rotation which is in agreement with the result obtained by Seth et al. [36]. Hall current tends to enhance fluid flow in both primary and secondary flow directions whereas ion-slip tends to enhance fluid flow in primary flow direction and it has reverse effect on the fluid flow in secondary flow direction. Rotation tends to retard fluid flow in the primary flow direction and it has reverse effect on the fluid flow in the secondary flow direction whereas magnetic field tends to retard fluid flow in both the primary and secondary flow directions. Permeability tends to enhance fluid flow in both primary and secondary flow directions whereas suction tends to enhance fluid flow in primary flow direction and injection has reverse effect on it. Fluid flow in the primary flow direction is getting enhanced as time progresses when $0.25 \leq t^* \leq 0.50$ whereas it has reverse effect on the fluid flow in primary flow direction when $0.50 < t^* \leq 1.0$. Fluid flow in secondary flow direction is enhanced as time passes.

Hall current tends to reduce primary shear stress at the moving plate and it has reverse effect on the secondary shear stress at the moving plate

whereas ion-slip tends to enhance both the primary and secondary shear stresses at the moving plate. Rotation tends to reduce both the primary and secondary shear stresses at the moving plate. Magnetic field tends to enhance primary shear stress at the moving plate and secondary shear stress at the moving plate when $3 < K^2 \leq 4$ whereas it has reverse effect on the secondary shear stress at the moving plate when $1 \leq K^2 \leq 3$. Permeability tends to reduce primary shear stress at the moving plate and it has reverse effect on the secondary shear stress at the moving plate. Both the time and pressure gradient tend to enhance both the primary and secondary shear stresses at the moving plate.

Acknowledgements

Authors are thankful to the Editor and Reviewer for their valuable comments and suggestions to improve the quality of the research paper. One of the authors S. Ghousia Begum is thankful to University Grant Commission (UGC), New Delhi for providing financial assistance to carry-out this research work.

References

[1] Z. Abbas, M. Sajid and T. Hayat, *MHD boundary-layer flow of an upper convected Maxwell fluid in porous channel*, Theo. Comp. Fluid Dyn. **20** (2006) 229–238.

[2] S. Ahmed and A.J. Chamkha, *Hartmann Newtonian radiating MHD flow for a rotating vertical porous channel immersed in a Darcian Porous Regime*, Int. J. Num. Methods Heat Fluid Flow **24(7)** (2014) 1454–1470.

[3] H.A. Attia, *Unsteady Couette flow with heat transfer considering ion-slip*, Turkish J. Phys. **29** (2005) 379–388.

[4] J. Bear, *Dynamics of Fluids in Porous Media*, Dover Pub., New York, 1988.

[5] O.A. Beg, H.S. Takhar, J. Zueco, A. Sajid and R. Bhargava, *Transient Couette flow in a rotating non-Darcian porous medium parallel plate configuration: network simulation method solutions*, Acta Mech. **200** (2008) 129–144.

[6] O.A. Beg, J. Zueco and H.S. Takhar, *Unsteady magnetohydrodynamic Hartmann-Couette flow and heat transfer in a Darcian channel with Hall current, ion-slip, viscous and Joule heating effects: Network numerical solutions*, Comm. Nonlinear Sci. Num. Sim. **14** (2009) 1082–1097.

[7] P. Chandran, N.C. Sacheti and A.K. Singh, *Effect of rotation on unsteady hydromagnetic Couette flow*, Astrophys. Space Sci. **202** (1993) 1–10.

[8] D.S. Chauhan and R. Agrawal, *Effects of Hall current on MHD Couette flow in a channel partially filled with porous medium in a rotating system*, Meccanica **47(2)** (2012) 405–421.

[9] K.R. Cramer and S.I. Pai, *Magnetofluid-dynamics for Engineers and Applied Physicists*, McGraw-Hill Book Comp., New York, 1973.

[10] S. Das, S.L. Maji, M. Guria and R.N. Jana, *Unsteady MHD Couette flow in a rotating system*, Math. Comp. Model. **50** (2009) 1211–1217.

[11] L. Debnath, *On Ekman and Hartmann boundary layers in a rotating fluid*, Acta Mech. **18** (1973) 333–341.

[12] L. Debnath, *Resonant oscillations of a porous plate in an electrically conducting rotating viscous fluid*, Physics of Fluids **17** (1974) 1704–1706.

[13] S. Guchhait, S. Das, R.N. Jana and S.K. Ghosh, *Combined effects of Hall current and rotation on unsteady Couette flow in a porous channel*, World J. Mech. **1** (2011) 87-199.

[14] M. Guria, S. Das, R.N. Jana and S.K. Ghosh, *Oscillatory Couette flow in the presence of inclined magnetic field*, Meccanica **44** (2009) 555–564.

[15] T. Hayat, N. Ahmad, M. Sajid and S. Asghar, *On the MHD flow of second grade fluid in a porous channel*, Comp. Math. Appl. **54** (2007) 407–414.

[16] T. Hayat, S. Hutter, S. Asghar and A.M. Siddiqui, *MHD flows of an Oldroyd-B fluid*, Math. Comp. Model. **36** (2002) 987-995.

[17] T. Hayat, S.B. Khan and M. Khan, *Exact solution for rotating flows of a generalized Burgers fluid in a porous space*, Appl. Math. Model. **32** (2008) 749–760.

[18] T. Hayat, S. Nadeem and S. Asghar, *Hydromagnetic Couette-flow of a Oldroyd-B fluid in a rotating system*, Int. J. Eng. Sci. **42** (2004) 65–78.

[19] R. Hide and P.H. Roberts, *Hydromagnetic flow due to an oscillating plane*, Rev. Mod. Phys. **32** (1960) 799–806.

[20] B.K. Jha and C.A. Apere, *Combined effect of Hall and ion-slip currents on unsteady MHD Couette flows in a rotating system*, J. Phys. Soc. Japan **79** (2010) 104401 (9 pages).

[21] B.K. Jha and C.A. Apere, *Magnetohydrodynamic free convective Couette flow with suction and injection*, ASME J. Heat Transfer **133 (9)** (2011) 092501 (12 pages).

[22] B.K. Jha and C.A. Apere, *Time-dependent MHD Couette flow of rotating fluid with Hall and ion-slip currents*, Appl. Math. Mech. **33(4)** (2012) 399–410.

[23] O.D. Makinde, O.A. Beg and H.S. Takhar, *Magnetohydrodynamic viscous flow in a rotating porous medium cylindrical annuls with an applied radial magnetic field*, Int. J. Appl. Math. Mech. **5(6)** (2009) 68–81.

[24] N.W. McLachlan, *Complex Variable and Operational Calculus with Technical Applications*, Cambridge University Press, New York, 1947.

[25] R.C. Meyer, *On reducing aerodynamic heat-transfer rates by magnetohydrodynamic technique*, J. Aerospace Sci. **25** (1958) 561–572.

[26] S.P. Mishra and J.C. Muduli, *Unsteady flow through two porous flat walls in the presence of a magnetic field*, Rev. Roum. des Sci. Tech. Serie de Mech. Appl. **25** (1980) 21–27.

[27] R.S. Nanda and H.K. Mohanty, *Hydromagnetic flow in a rotating channel*, Appl. Sci. Res. **24** (1971) 65–78.

[28] D.R.V. Prasad Rao, D.V. Krishna and L. Debnath, *Combined effect of free and forced convection on MHD flow in a rotating porous channel*, Int. J. Math. Math. Sci. **5** (1982) 165–182.

[29] G. Sarojamma and D.V. Krishna, *Transient hydromagnetic convective flow in a rotating channel with porous boundaries*, Acta Mech. **40** (1981) 277–288.

[30] G.S. Seth, Md.S. Ansari and R. Nandkeolyar, *Unsteady hydromagnetic Couette flow within porous plates in a rotating system*,Adv. Appl. Math. Mech. **2(3)** (2010) 286–302.

[31] G.S. Seth, Md.S. Ansari and R. Nandkeolyar, *Unsteady hydromagnetic Couette flow induced due to accelerated movement of one of the porous plates of the channel in a rotating system*, Int. J. Appl. Math. Mech. **6(7)** (2010) 24–42.

[32] G.S. Seth, Md.S. Ansari and R. Nandkeolyar, *Effects of rotation and magnetic field on unsteady Couette flow in a porous channel*, J. Appl. Fluid Mech. **4(2)** (2011) 95–103.

[33] G.S. Seth and R.N. Jana, *Unsteady hydromagnetic flow in a rotating channel with oscillating pressure gradient*, Acta Mech. **37** (1980) 29–41.

[34] G.S. Seth, R.N. Jana and M.K. Maiti, *Unsteady hydromagnetic Couette flow in a rotating system*, Int. J. Eng. Sci. **20** (1982) 989–999.

[35] G.S. Seth and J.K. Singh, *Effects of Hall current and rotation on unsteady MHD Couette flow in a porous channel in the presence of a moving magnetic field*, J. Nature Sci. Sustainable Tech. **5(4)** (2011) 263–283.

[36] G.S. Seth, J.K. Singh and G.K. Mahato, *Effects of Hall current and rotation on unsteady hydromagnetic Couette flow within a porous channel*, Int. J. Appl. Mech. **4(2)** (2012) 1250015 (25 pages).

[37] K.D. Singh, *An oscillatory hydromagnetic Couette flow in a rotating system*, ZAMM **80** (2000) 429–432.

[38] K.D. Singh and R. Pathak, *Effect of rotation and Hall current on mixed convection MHD flow through a porous medium filled in a vertical channel in presence of thermal radiation*, Ind. J. Pure Appl. Phys. **50** (2012) 77–85.

[39] A.K. Singh, N.C. Sacheti and P. Chandran, *Transient effects on magnetohydrodynamics Couette flow with rotation: Accelerated motion*, Int. J. Eng. Sci. **32** (1994) 133–139.

[40] V.M. Soundalgekar, N.V. Vighnesam and H. S. Takhar, *Hall and ion-slip effects in the MHD Couette flow with heat transfer*, IEEE Trans. Plasma Sci. **7** (1979) 178–182.

[41] P. Sulochana, *Hall effects on unsteady MHD three dimensional flow through a porous medium in a rotating parallel plate channel with effect of inclined magnetic field*, American J. Comp. Math. **4** (2014) 396–405.

[42] Y. Wang and T. Hayat, *Hydromagnetic rotating flow of fourth-order fluid past a porous plate*, Math. Methods Appl. Sci. **27** (2004) 477–496.